

Test of a proton radiography prototype with 62MeV protons

David Menichelli¹, Mara Bruzzi, Marta Bucciolini, Stefania Pallotta, Monica Scaringella, Cinzia Talamonti, Mauro Tesi

Università degli Studi di Firenze, Firenze (Italy)

Giuliana Candiano, Giuseppe A. P. Cirrone, Giacomo Cuttone

INFN- Laboratori Nazionali del Sud, Catania (Italy)

Carlo Civinini, Mirko Brianzi

INFN- Sezione di Firenze, Firenze (Italy)

Domenico Lo Presti, Valeria Sipala

Università degli Studi di Catania, Catania (Italy)

Livia Marrazzo

Azienda Ospedaliero-Universitaria Careggi, Firenze (Italy)

Nunzio Randazzo

INFN- Sezione di Catania, Catania (Italy)

The Italian PRoton IMAGING (PRIMA) collaboration is developing a Proton Computed Radiography (pCR) apparatus. It should be considered a first step toward Proton Computed Tomography (pCT), which is expected to be a valuable tool to directly measure stopping power distribution of tissues and to improve the quality of treatment planning in proton therapy. The pCR apparatus includes a tracker (based on a set of identical tracker modules, each including a silicon microstrip detector) to measure proton trajectory and a calorimeter (made of four YAG:Ce optically separated crystals) to measure residual energy. Two tracker modules can be assembled in a x-y plane, capable to measure the local coordinates of the incoming proton. The first assembled x-y plane has been recently coupled to the calorimeter, and this system was tested with 62MeV protons. Results from this experiment are presented in this contribution.

9th International Conference on Large Scale Applications and Radiation Hardness of Semiconductor Detectors-Rd09

Florence, Italy

30 September - 2 October 2009

¹ Speaker. Address: INFN Firenze, Via B. Rossi 1, 50019 Sesto Fiorentino (Italy). Tel. +39 055 4572688. Electronic address: david.menichelli@cern.ch.

1. Introduction

One of the main advantages in using protons and light ions to treat tumors is the possibility to tightly shape the radiation dose to the target volume, thanks to the peculiarities of the interaction of hadrons with matter. However, the spatial accuracy of proton therapy is still presently limited by the uncertainty in stopping power distribution, which is calculated from the photon attenuation coefficients measured by X-ray tomography [1]. This uncertainty could be reduced by directly measuring stopping powers with a proton beam, by means of a proton tomography (pCT) apparatus [2],[3]. The aim of our project [4] is to design, manufacture and test a proton computed radiography (pCR) prototype for small objects analysis. Multiple images of the same object, taken at different angles (e.g. by using a rotating phantom), will be used to develop novel reconstruction algorithms, able to account for multiple Coulomb scattering and thus not entirely based on Monte Carlo simulations as in present times [5]. The final pCT system should be able to measure electron density with accuracies better than 1% and with a spatial resolution better than 1 mm. The main problem with pCT is that protons do not move along straight lines across the medium because of multiple Coulomb scattering. Anyway, single proton tracking is a promising way to collect as much as possible information in order to circumvent this difficulty [6], [7].

The pCR system presented in this paper has been designed to detect protons with initial kinetic energy high enough to transverse a human trunk (in the range 250 to 270MeV), with a particle rate of ~1MHz, in order to collect data within a time of the order of 1s, suitable to clinical demands. This device includes a tracker, based on silicon microstrip sensors, and a segmented calorimeter formed by four YAG:Ce crystals. The tracker measures proton trajectories, upstream and downstream the phantom, in terms of angle formed with beam axis and position in the transverse plane, while the calorimeter measures particle residual energy. These parameters are the input data necessary to calculate the protons most likely path. As a matter of fact, it has been recently proved that a semi-analytical algorithm [8] is suitable to determine the most likely path of protons and to account for the blurring effect introduced in proton radiographic images by Coulomb scattering [9].

Both the tracker components and the calorimeter crystals have been extensively tested with charged particles [10]-[14]. A single YAG:Ce crystal was tested with 62MeV protons at INFN-LNS (Catania, Italy) while the 4-crystals device was tested with 200MeV protons at Loma Linda University Medical Center (Loma Linda, CA, USA). The silicon sensor and its readout electronics were tested with β particles from a ^{90}Sr Source at INFN Florence and 62MeV protons at INFN-LNS. The first measurements carried out by coupling silicon sensors to the calorimeter are presented in this contribution.

2. System under test

An overview of the complete pCR system design is described in Figure 1. A detailed description can be found in [10]-[13]. It includes a tracker and a segmented calorimeter (a). The tracker is composed of 4 x-y planes (p1 to p4) capable to measure x and y coordinates of

particle trajectory. Planes p1 and p2 measure entrance angle and position; the object under study (a phantom in this case) is placed in the gap between planes p2 and p3; planes p3 and p4 measure exit angle and position. The distance between entrance (or exit) planes is about 1cm and could be changed to optimize the measurement quality. Beyond the last plane (p4), protons stop inside the calorimeter (a), which measures particle residual energy.

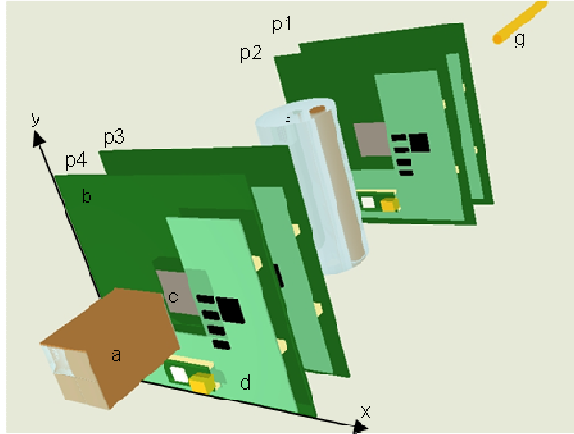


Figure 1: architecture of the proton computed radiography system, including four x-y planes (p1-p4) and a segmented calorimeter (a).



Figure 2: photograph of the tracker module. The L-shaped digital board sits on top of the front end board. The silicon sensor is placed on a squared hole in the center of the latter.

A x-y plane is composed of two identical tracker modules, each including a 256-channels silicon microstrip detector (c), analog front-end ASIC and digital electronics for data acquisition and transmission. The detector is processed from a 4" wafer and has an active area $51 \times 51 \text{ mm}^2$. The silicon detector, produced by Hamamatsu Photonics, is a 256-channels microstrip sensor obtained by implanting p^+ strips in a $200 \mu\text{m}$ thick n-type floating zone wafer with $\langle 100 \rangle$ crystal orientation. Strip pitch is $200 \mu\text{m}$. This sensor is designed to be operated in the range 100 to 200V reverse bias: full depletion voltage is less than 75V and the leakage current at 200V is less than 500 nA. Strips are AC coupled to the readout pads by an integrated capacitance of 280pF, and biased through a $1.25 \text{ M}\Omega$ polysilicon resistor.

One of the two tracker modules within the same x-y plane is flipped upside down and rotated by 90° to measure both the x and y local trajectory coordinates. Each tracker module includes two electronics boards: a front end board (b), carrying the silicon microstrip detector (c) and readout ASICs, and a tracker digital board (d), which communicates with the control terminal (PC) through an Ethernet connection. A photograph of a tracker module is shown in Figure 2.

The readout ASIC consists of 32 independent channels, including a charge sensitive amplifier, a shaper and a comparator suitable to produce a digital output by comparison with a threshold V_{th} . The threshold level of each front end board can be chosen independently of the others, and a fine threshold regulation through potentiometers can be made chip by chip. Thus the thresholds on a given board, expressed in Volts, are:

$$V_{th}^{(j)} = 1.650 + \Delta V_{th} - V_j \quad (1)$$

where $j=1\dots 8$ is the ASIC index, 1.650V is the quiescent level of shaper output, $(1.650+\Delta V_{th})$ is the threshold level set on the board and V_j is the fine regulation aimed to optimize the performances of the j^{th} chip.

The tracker digital board carries a low-cost FPGA with high input-output capabilities (Xilinx Spartan 3AN XC3S1400AN), a static RAM memory (composed of 4 1Mbit \times 16 static memories) and a commercial Ethernet unit (Memec V4Fx12 mini-module). The main role of the FPGA is to sample the 256 data lines from ASIC buffers, to implement pre-processing (including zero-suppression) and to store reduced data inside the memories. Data from about 400×10^3 events can be stored on board using the present firmware version.

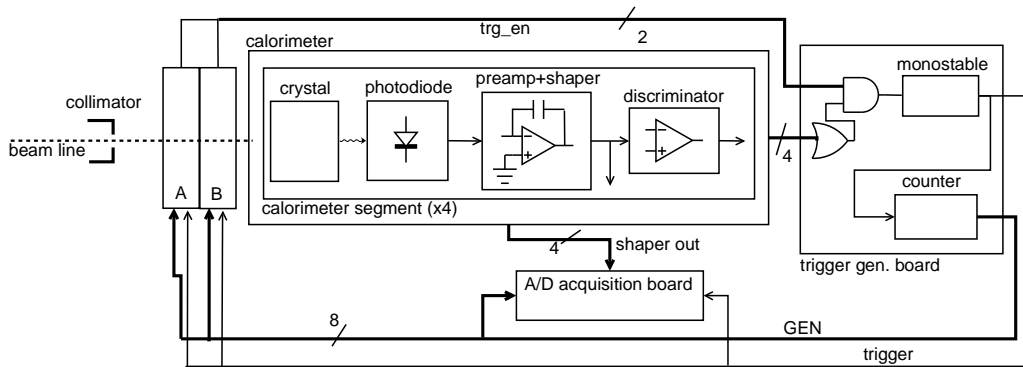


Figure 3: block scheme of experimental setup. A and B indicate the two tracker modules. Details about calorimeter and trigger generation are given. Trigger can be generated only if both the tracker modules are ready to acquire data and assert the trg_en lines.

Noise level can be made negligible if a proper threshold level is chosen. On the basis of electrical front-end board calibration and Monte Carlo simulations about the charge released by protons in silicon, we estimate [12] that it is possible to track protons in the energy range of interest (up to 250MeV) with high efficiency and low noise. In particular, a noise occupancy $<10^{-6}$ is obtained as long as $(\Delta V_{th}-V_j)>50\text{mV}$. In the case of protons with kinetic energy of 62MeV or less, the 99% efficiency is ensured for all channels if $\Delta V_{th}\leq 250\text{mV}$ ($\Delta V_{th}\leq 100\text{mV}$ in the case of 250MeV protons).

Each scintillating crystal has $30\times 30\text{ mm}^2$ cross section and is coupled to one photodiode. The analog outputs of photodiodes readout electronics are directly sampled by a commercial (14 bit, 50MHz maximum sampling frequency) acquisition board, in order to measure their maxima, which are proportional to the energy released in the crystals. These signals are used also to generate the trigger and the event number (GEN). The GEN is incremented by one at each trigger, and then attached to all data generated by tracker modules and by the calorimeter. GEN is used to merge offline data taken by the tracker and by the calorimeter.

The system actually tested in this work, which is described in Figure 3, included the calorimeter and one x-y plane (formed by tracker modules indicated here as A and B). Data have been measured using the Catania beam line at INFN-LNS (Laboratori Nazionali del Sud), at Catania, Italy. At this facility protons are accelerated by a superconducting cyclotron up to the kinetic energy of 62 MeV. When required, proton energy can be degraded placing absorbers along the beam line. Particle rates in the range 1-50 kHz have been used in our test. A

collimator was placed at the end of the beam pipe, upstream the x-y plane, while the calorimeter sited few centimeters downstream the plane.

3. Experimental results and discussion

An image of the 62 MeV beam, as measured by the x-y plane, is shown in Figure 4. Here the number of protons crossing the plane at a given x-y position is shown using false colors. About 100×10^3 events with a single cluster have been selected to generate this map. This image can be split in four regions (I-IV), according to the calorimeter crystal which generated the trigger. For instance, events in region I are recorded by tracker modules following a trigger generated by crystal no. I. Crystal no. III was not enabled to generate trigger during these measurements, thus data in the corresponding region are missing. Scattered protons crossing the microstrip sensors with large incidence angles do not hit the crystals and do not produce a trigger. For this reason, there is a region close to sensor border in which no events are recorded ($x > 180$, $y > 220$ or $y < 50$). A projection of the map along y axis is shown in Figure 5. A Gaussian fit is superimposed to the plot. The resulting standard deviation ($\sigma = 2.17\text{mm}$) is in good agreement with the collimator diameter (5 mm).

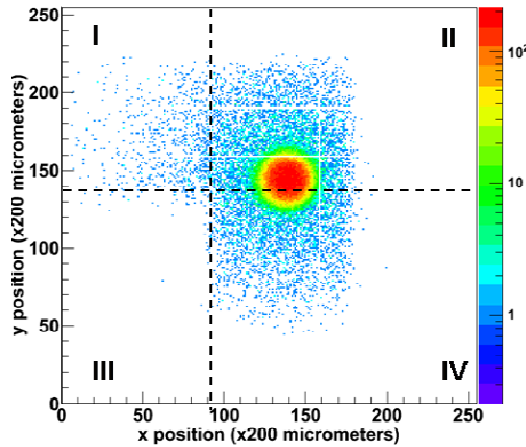


Figure 4: number of protons crossing a given x-y position. The position is given in term of strip index (strip pitch is $200\mu\text{m}$). Collimator diameter is 5.0mm. $\Delta V_{th} = 200\text{mV}$.

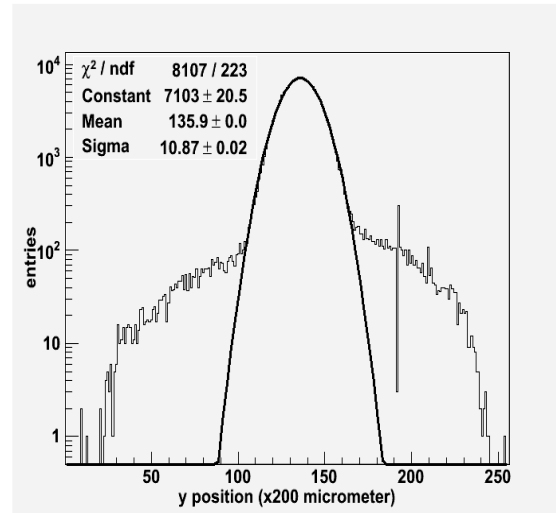


Figure 5: projection of the map shown in Figure 3 along y axis. A Gaussian fit of the main component is superimposed to the plot.

A map of events triggered by crystals II and IV, denoting the correct correlation between tracker and calorimeter data, is shown in Figure 6. In this case the relative position of beam axis, x-y plane and calorimeter is different from that of Figure 3. Moreover in this case the collimator was removed from the beam pipe. Events triggered by crystal II (IV) are plotted as red (black) scatters. The projection of these data along y axis is shown in Figure 7, where the number of events with a given y coordinate triggered by crystal II (IV) is plotted with a solid red (black) line.

The ASICs on the tracker front end board produce a digital output whose duration $T(V_{th}, E)$ is related to the charge released by particles with kinetic energy E in the silicon sensor. This

duration can be measured by the FPGA on the tracker digital board, and used to improve the calorimeter reading. The dependency of most probable duration on ASIC threshold is shown in Figure 8. Both the tracker modules exhibit a linear dependency with the same slope (-1.10ns/mV) but different intercepts (670 ns and 730 ns). This is due the fact that a different threshold regulation was made on the two modules to optimize their noise performances. In Figure 9, pulse duration measured at $\Delta V_{\text{th}}=200\text{mV}$ is plotted versus protons kinetic energy. In this case the dependency is not linear because of the non-linear response of chips.

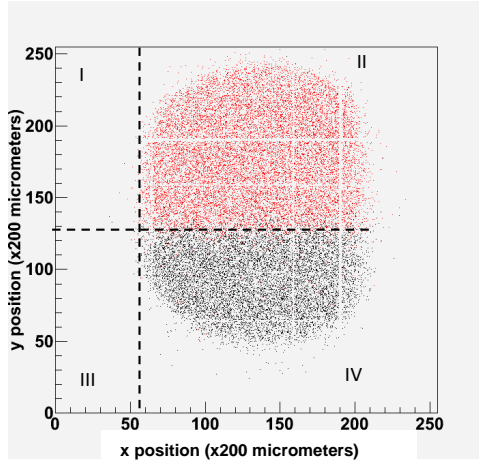


Figure 6: map of events triggered by crystals II (red) and IV (black). $\Delta V_{\text{th}}=200\text{mV}$, 62MeV initial kinetic energy. The collimator was removed from the beam pipe.

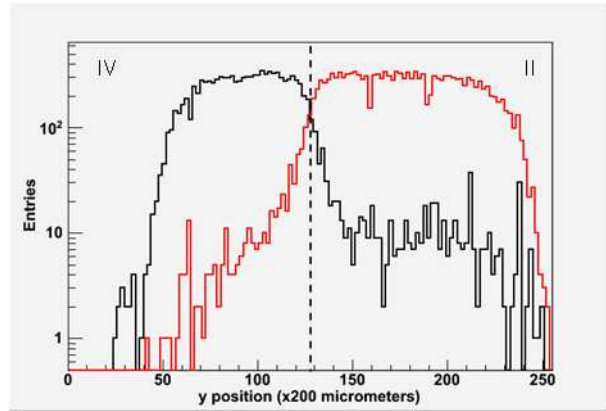


Figure 7: projection of data from Figure 6 along y axis. The histogram of events triggered by crystal IV (II) is plotted with a black (red) solid line.

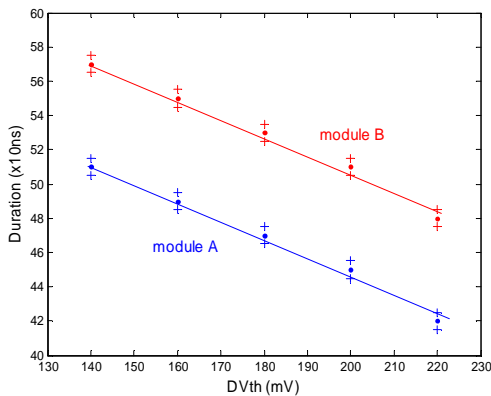


Figure 8: Most probable value of pulse duration T versus ASIC threshold ΔV_{th} at fixed proton kinetic energy ($E=62\text{MeV}$). Duration is expressed in terms of clock cycles (clock period is 10ns).

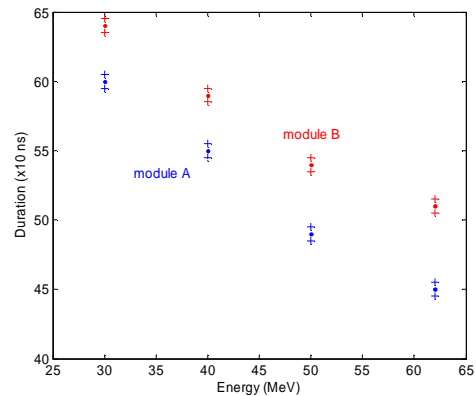


Figure 9: Most probable value of pulse duration T versus proton kinetic energy E at fixed threshold ($\Delta V_{\text{th}}=200\text{mV}$). Duration is expressed in terms of clock cycles (clock period is 10ns).

4. Conclusions

A system for proton radiography has been designed. It includes: i) a tracker based on Si microstrip detectors and ii) a segmented YAG:Ce calorimeter. Previously, all the components had been manufactured and tested separately with protons of various energies. The first test with

protons at INFN-LNS of a tracker x-y plane coupled to the calorimeter has been reported in this contribution. Protons in the energy range 20-62MeV, with a particle rate in the range 1-50 kHz, were measured. It has been proved that data from various tracker modules and from the calorimeter can be correlated offline by using GEN tag, and that an unambiguous event building can be carried out. Moreover, results obtained with previous experiments in a preliminary form have been improved using a more significant statistics. In particular it has been proved that a) the beam profile can be correctly measured and b) the response $T(V_{th}, E)$ of tracker ASIC has a linear dependence on threshold voltage V_{th} at a fixed proton kinetic energy E .

The assembling of the complete tracker (with 4 x-y planes) is presently under way, and a beam test with 200MeV protons at Essen WPC is scheduled in 2010. The development of a fast readout electronics for the calorimeter, suitable to increase the particle rate toward the target value of 1MHz, is under way as well.

Acknowledgements

This work was supported by INFN PRIMA experiment.

References

- [1] U. Schneider, E. Pedroni and A. Lomax, *The calibration of CT Hounsfield units for radiotherapy treatment planning*, Phys. Med. Biol. **41** (111) 1996.
- [2] P. Zygmanski, K. P. Gall, M. S. Z. Rabin and S. J. Rosenthal, *The measurement of proton stopping power using proton-cone-beam computed tomography*, Phys. Med. Biol. **45** (511) 2000.
- [3] R. Schulte et al., *Conceptual design of a proton computed tomography system for applications in proton radiation therapy*, IEEE Trans. Nucl. Sci. **51** (866) 2004.
- [4] G.A.P. Cirrone et al., *The Italian project for a proton imaging device*, Nucl. Instr. and Meth. A **576** (194) 2007.
- [5] T. Li, Z. Liang, J. V. Singanallur, T. J. Satogata, D. C. Williams, and R. W. Schulte, *Reconstruction for proton computed tomography by tracing proton trajectories: A Monte Carlo study*, Med. Phys. **33** (699) 2006.
- [6] U. Schneider and E. Pedroni, *Multiple Coulomb scattering and spatial resolution in proton radiography*, Med. Phys., **21** (1657) 1994.
- [7] G. A. P. Cirrone et al., *Monte Carlo Studies of a Proton Computed Tomography System*, IEEE Trans. Nucl. Sci., **54** (1487) 2007.
- [8] D. C. Williams, *The most likely path of an energetic charged particle through a uniform medium*, Phys. Med. Biol., **49** (2899) 2004.
- [9] C. Talamonti et al., *Proton Radiography for clinical applications*, Nucl. Instr. and Meth. A, **612** (571) 2009. Doi:10.1016/j.nima.2009.08.040.
- [10] D. Menichelli et al., *Development of a Proton Computed Radiography Apparatus*, in 2008 IEEE Nuclear Science Symposium Conference Record, p.5600, 2008.
- [11] D. Menichelli et al., *Characterization of a silicon strip detector and a YAG:Ce calorimeter for a proton computed radiography apparatus*, IEEE Trans. Nucl. Sci., **57** (8), 2010. Doi: 10.1109/TNS.2009.2031869.
- [12] V. Sipala et al., *A proton imaging device: design and realization status*, Nucl. Instr. and Meth. A, **612** (566), 2010; doi:10.1016/j.nima.2009.08.029.
- [13] D. Menichelli et al., *Assembling and Test of a Proton Computed Radiography Apparatus*, in 2009 IEEE Nuclear Science Symposium Conference Record, p.4181; doi 10.1109/TNS.2009.2031869.
- [14] C. Civinini et al., *Towards a Proton Imaging System*, Nucl. Instr. and Meth. A, in press. Available online 11 March 2010. Doi:10.1016/j.nima.2010.03.079.